ACS SyntheticBiology

Research Article

pubs.acs.org/synthbio

In Vitro Membrane Protein Synthesis Inside Cell-Sized Vesicles Reveals the Dependence of Membrane Protein Integration on Vesicle Volume

Haruka Soga,[†] Satoshi Fujii,[‡] Tetsuya Yomo,[‡,§] Yasuhiko Kato,[†] Hajime Watanabe,[†] and Tomoaki Matsuura*[,†,‡]

[†]Department of Biotechnology, Graduate School of Engineering, Osaka University, 2-1 Yamadaoka, Suita, Osaka, Japan

[‡]Exploratory Research for Advanced Technology, Japan Science and Technology Agency, 1-5 Yamadaoka, Suita, Osaka, Japan

[§]Department of Bioinformatic Engineering, Graduate School of Information Science and Technology, Osaka University, 1-5 Yamadaoka, Suita, Osaka, Japan

Supporting Information

ABSTRACT: Giant unilamellar vesicles (GUVs) are vesicles >1 μm in diameter that provide an environment in which the effect of a confined reaction volume on intravesicular reactions can be investigated. By synthesizing EmrE, a multidrug transporter from *Escherichia coli*, as a model membrane protein using a reconstituted *in vitro* transcription−translation system inside GUVs, we investigated the effect of a confined volume on the synthesis and membrane integration of EmrE. Flow cytometry was used to analyze multiple properties of the vesicles and to quantify EmrE synthesis inside GUVs composed of only 1-palmitoyl-2-oleoyl-sn-glycero-3-phosphocholine. We found that EmrE was synthesized and integrated into the GUV membrane in its active form. We also found that the ratio of membrane-integrated EmrE to total synthesized EmrE increased with decreasing vesicle volume; this finding is explained by the effect of an increased surface-area-to-volume ratio in smaller vesicles. *In vitro* membrane synthesis inside GUVs is a useful approach to study quantitatively the properties of membrane proteins and their interaction with the membrane under cell-mimicking environments.

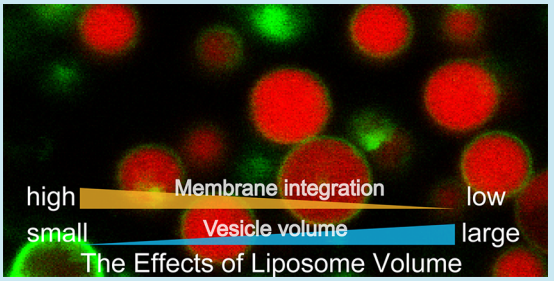

KEYWORDS: *cell-free protein synthesis, multidrug transporter, giant unilamellar vesicles, membrane curvature, surface-area-to-volume ratio*

Membrane proteins account for 20−25% of all open reading frames in the genome, and more than 50% of currently available pharmaceuticals target membrane proteins.[1,2] Membrane protein research is therefore an important research field; however, there are many obstacles to the analysis and preparation of these proteins. The natural abundance of membrane proteins is typically too low to allow their detailed characterization, and overexpression of these proteins often results in low yield, cell toxicity, and aggregation. In addition, because membrane proteins are naturally embedded in the lipid membrane, their isolation requires a specific environment. *In vitro* transcription−translation systems (IVTTs) are useful tools for overcoming such difficulties.[3−5] Because protein synthesis using an IVTT is disconnected from cell growth[6] and constitutes an open system, the reaction can be performed in the presence of detergents, lipids, and nanodiscs, resulting in the synthesis of membrane proteins in their active form in a few hours[3]

One emerging technique in *in vitro* membrane protein synthesis involves the synthesis of proteins inside cell-sized liposomes that are larger than 1 μm in diameter.[7−9] This method differs from the protein synthesis that occurs in the presence of detergents or lipids in the following ways. First, the cell-sized vesicles mimic the cellular environment. For example, the vesicles provide an environment with negative curvature. Membrane curvature plays an important role in enabling membrane protein localization *in vivo*,[10−12] and *in vitro* assays that investigate the effect of both the positive and negative membrane curvature are possible with cell-sized vesicles. Second, membrane proteins synthesized inside cell-sized vesicles can be detected at the single-vesicle level using flow cytometry (FCM) and/or microscopy;[13] these methods allow, for example, the analysis of the relationship between vesicle volume and membrane protein function.[14,15] Third, the synthesis of membrane proteins inside vesicles also allows gene screening.[16,17] If the activity of the membrane protein can be converted to a fluorescent signal in the vesicle, then genes that encode membrane proteins with desired properties can be screened from a gene pool using fluorescence-activated cell

Special Issue: Cell-Free Synthetic Biology

Received: July 31, 2013
Published: December 5, 2013

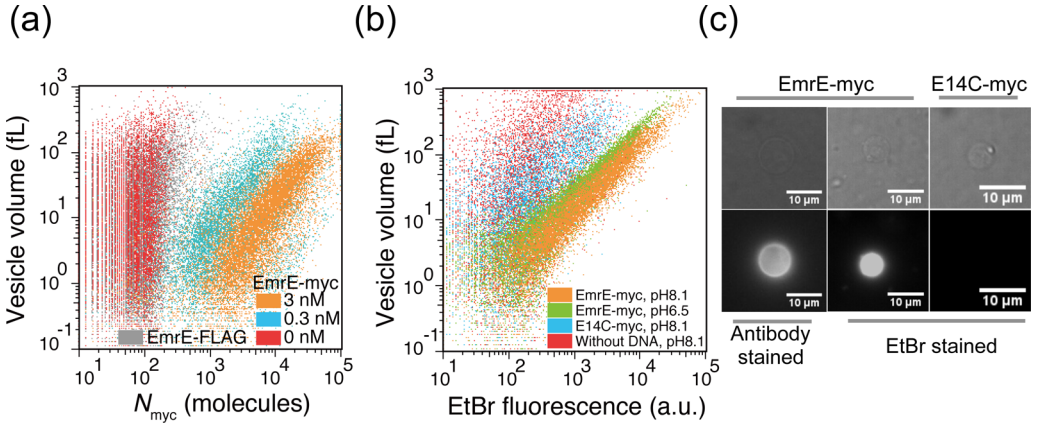

Figure 1. EmrE synthesis inside GUVs using the PURE system. (a) Two-dimensional FCM analysis of EmrE-displaying GUVs with different DNA concentrations (0, 0.3, and 3 nM of EmrE-myc and 1 nM of EmrE-FLAG). To reduce the complexity of the plot, the data for 1 nM DNA are not shown. The relationship between the vesicle volume and N_{myc}, which is the number of membrane-integrated EmrE molecules with the myc-tag facing the outside of the vesicle, is shown. (b) Two-dimensional FCM analysis for the EtBr transport activity of EmrE-displaying vesicles. (c) Representative microscopy image of EmrE-displaying GUVs. The upper and lower rows are bright-field and fluorescence images, respectively.

sorting (FACS).[18,19] Despite the favorable properties of this method, only a limited number of membrane proteins[7,9] have been synthesized inside liposomes, none of which are transporters, which constitute a large proportion of membrane proteins.

In this study, we demonstrate that EmrE, a multidrug transporter from *Escherichia coli*, can be synthesized in its active form inside giant unilamellar vesicles (GUVs) using the *E. coli*-based reconstituted PURE IVTT system.[20] EmrE forms an antiparallel dimer that transports toxic compounds (e.g., ethidium bromide (EtBr) and acriflavine) from inside to outside the cell via the coupled reverse transport of protons.[21,22] We found that EmrE can be integrated into a GUV membrane that consists of 1-palmitoyl-2-oleoyl-sn-glycero-3-phosphocholine (POPC) and can transport EtBr against the pH gradient. In addition, by quantifying synthesized and membrane-integrated EmrE in GUVs of different sizes, we found that a higher fraction of EmrE was integrated into the membrane of smaller vesicles; this finding is quantitatively explained by the effect of the increased surface-area-to-volume ratio in smaller vesicles. Finally, we discuss the applications of membrane protein synthesis inside GUVs.

RESULTS AND DISCUSSION

EmrE Synthesis Inside Cell-Sized Vesicles. We first investigated whether EmrE could be synthesized inside vesicles and inserted into the phospholipid membrane. We encapsulated the PURE system with DNA encoding EmrE into GUVs prepared using the water-in-oil (w/o) emulsion-transfer method.[7,23] We performed the investigation with one of the simplest lipid compositions (i.e., 100% POPC). Note that with our preparation method[24] protein synthesis occurred only inside the vesicles, as there were no macromolecules (e.g., ribosomes and elongation factors) in the outer (extravesicular) solution. The vesicles were prepared at 4 °C to prevent EmrE synthesis from occurring during the preparation steps and were then incubated for 3 h at 37 °C. Three hours is the time at which the PURE system has nearly terminated because of the inactivation of the system.[20]

We used a DNA construct that encodes EmrE with a myc-tag at the C-terminus of EmrE (EmrE-myc). EmrE contains four transmembrane regions and functions as an antiparallel dimer.[21,22] Therefore, if integrated into the membrane with the correct topology, then the myc-tag of EmrE-myc should be available from both sides of the membrane. EmrE-myc was synthesized using different concentrations of DNA (0, 0.3, 1, and 3 nM) and stained with an Alexa Fluor 488 (AF488)-labeled anti-myc antibody followed by FCM analysis. The amount of EmrE with the myc-tag present on the outer side of the vesicle (N_{myc}) was estimated from the AF488 fluorescence, and the vesicle volume (V) was estimated from the transferrin–Alexa Fluor 647 conjugate (TA647) fluorescence included at 1 μM in the reaction mixture. The details of these conversions are described in the Methods section. The 2D FCM analysis of N_{myc} versus V indicated that more EmrE was integrated into the membrane at higher DNA concentrations (Figure 1a). In addition, the vesicles that displayed EmrE with a FLAG-tag at the C-terminus (EmrE-FLAG) demonstrated a similar result as those without DNA (Figure 1a). These results indicate that EmrE was synthesized inside the vesicle and inserted into the POPC membrane, as confirmed by fluorescence microscopy (Figure 1c). Increasing the concentration of the anti-myc antibody used for staining did not increase the signal (data not shown), indicating that the amount of antibody used was sufficient to stain nearly all of the myc-tags on the vesicle.

EtBr Transport by EmrE-Displaying Vesicles. We next aimed to investigate whether the EmrE present on the membrane was functional. We used EtBr as a model substrate because of its ability to emit fluorescence once transported into the vesicle, given that it binds to the rRNA, tRNA, and mRNA present only inside the vesicles.

After EmrE synthesis, EtBr was added to the outer solution, a pH gradient between the inner (pH 7.6) and outer solution (pH 6.8 or 8.1) was established, and the vesicles were analyzed using FCM (Figure 1b). EtBr is transported by EmrE via the coupled reverse transport of protons, and, indeed, EtBr fluorescence was higher when the pH of the outer solution was 8.1 compared with that at pH 6.8. Furthermore, EmrE-myc demonstrated significantly higher EtBr fluorescence than an inactive mutant (E14C[25]) and vesicles without DNA (Figures 1b and S1). These results were confirmed using fluorescence microscopy (Figure 1c). EmrE synthesized inside the vesicles not only was inserted into the membrane but also exhibited

dx.doi.org/10.1021/sb400094c | *ACS Synth. Biol.* 2014, 3, 372–379

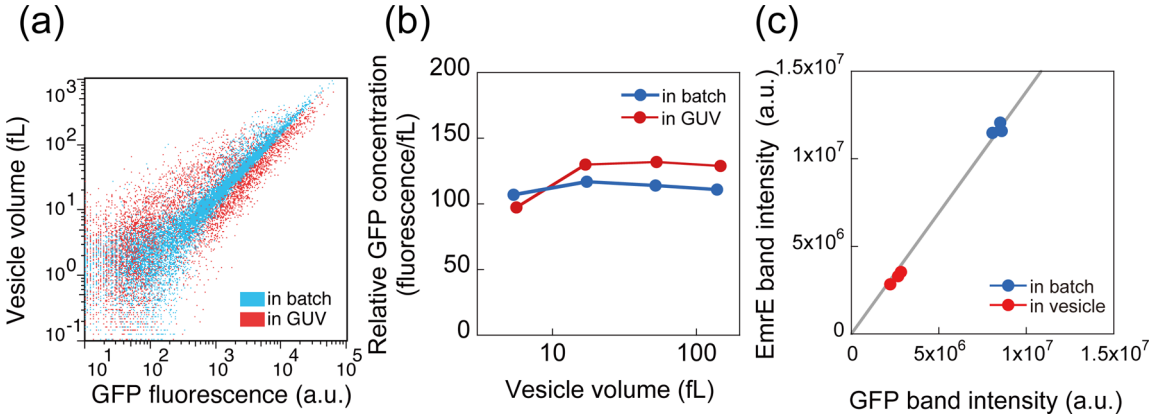

Figure 2. GFP and EmrE synthesis inside the GUVs and in batch. (a) Two-dimensional FCM analysis of GFP- and EmrE-synthesizing GUVs. The relationship between the vesicle volume and GFP fluorescence is shown. A DNA mixture of the genes encoding GFP and EmrE was prepared at a molar ratio of 1:1 (0.5 nM each) and used as a template for IVTT. The *in vitro* protein synthesis was performed inside the GUVs or in batch, and the product was subsequently encapsulated inside the GUVs, which were then subjected to FCM analysis. (b) Dependence of the relative concentration of GFP synthesized inside the GUV on the vesicle volume when EmrE is coexpressed and its comparison to the yield in batch synthesis. These results were obtained from the results shown in panel a. The vesicles were classified into groups with V values of 2.15−10, 10−46.4, 46.4−215, and 215−1000 fL. Subsequently, the median value of the GFP concentration and V for each group was calculated and plotted. Although the mechanism remains to be elucidated, the average concentration of GFP inside GUVs were nearly identical to those in batch, whereas the variability was greater inside GUVs. (c) Ratio of GFP and EmrE synthesized inside the vesicle or in batch. *In vitro* protein synthesis was performed with ^{35}S-methionine using a DNA mixture of the genes encoding GFP and EmrE at a molar ratio of 1:1 (0.5 nM each), and the band intensity was obtained from autoradiography of the SDS polyacrylamide gel. The results of three independent samples are shown. The solid line indicates the fit using a linear equation with an intercept of zero.

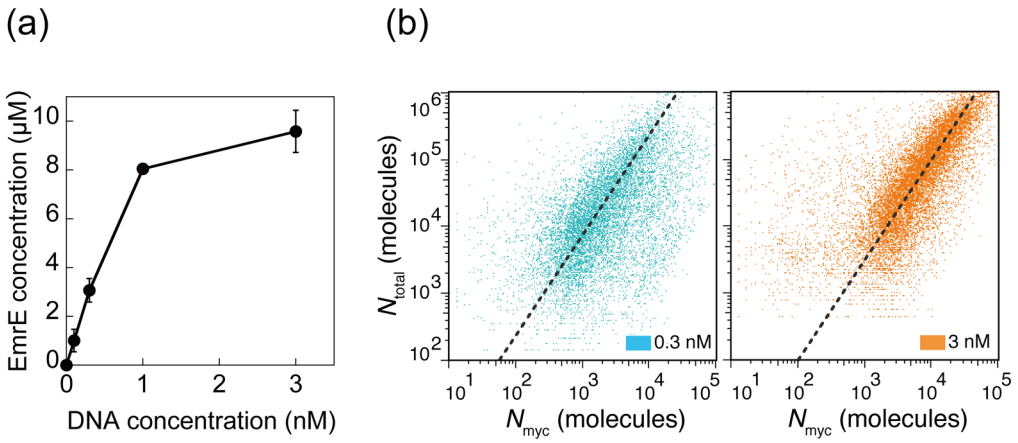

Figure 3. Total amount of EmrE synthesized in each vesicle. (a) Concentrations of synthesized EmrE, $[E]_0$, in a batch reaction with different DNA concentrations after a 3 h incubation at 37 °C. ^{35}S-Met was incorporated into the synthesized protein, and the band intensity of the autoradiograph of the SDS polyacrylamide gel was analyzed. The average and the standard deviation of three independent samples are shown. (b) Two-dimensional FCM analysis indicating the relationship between N_{total} and N_{myc} at different DNA concentrations (0.3 and 3 nM). N_{total} of each vesicle was obtained using the equation $N_{total} = [E]_0 V$. The dashed line indicates the fit of the data with the curve $\log N_{total} = 1.5 \log N_{myc} + c$, where c is the fitting parameter. The fit using $\log N_{total} = n \log N_{myc} + c$, where n and c are the fitting parameters, resulted in values of $n = 1.58$ and $c = -0.93$ for 0.3 nM DNA and $n = 1.62$ and $c = -1.48$ for 3 nM DNA.

transport activity, indicating that the EmrE on the membrane existed in its functional form as an antiparallel homodimer.

Quantification of Intravesicular EmrE Synthesis. To elucidate the dependence of EmrE synthesis on vesicle volume, we estimated two values, N_{total} and N_{myc}, which represent the total number of EmrE molecules synthesized inside the vesicle with volume, V, and the number of membrane-integrated EmrE molecules with the myc-tag facing outside of the vesicle, respectively.

N_{myc} was estimated as previously described (Figure 1a). One of the most popular strategies to quantify the amount of expressed protein (e.g., N_{total}) is to fuse the protein of interest with a sequence for a fluorescent tag such as GFP. EmrE is a protein that is not suitable for this approach because the EmrE synthesized inside the GUV has at least two fates: membrane integration or aggregation. It is likely that these two fates will exhibit different GFP fluorescence intensities per molecule and thus the total GFP fluorescence intensity does not necessarily reflect the total yield of the synthesized product. Therefore, to estimate N_{total}, we employed the following strategy.

We began by measuring the difference between the protein synthesis in GUVs and in batch. A DNA mixture of the genes encoding GFP and EmrE was prepared at a molar ratio of 1:1 and was used as a template for IVTT. The synthesis was performed inside the GUVs or performed in batch, and the product was subsequently encapsulated inside the GUVs. Two

dx.doi.org/10.1021/sb400094c | *ACS Synth. Biol.* 2014, 3, 372−379

vesicles were subjected to FACS analysis (Figure 2a). There was no significant difference between the yield of GFP in GUVs and in batch even when EmrE was coexpressed. Furthermore, the GFP concentration, [GFP], inside the vesicle was constant irrespective of the vesicle volume (Figure 2b). Therefore, the number of GFP molecules (N_{GFP}) inside a vesicle with volume V demonstrated the following relationship: $N_{GFP} = [GFP]V$, where [GFP] is the value obtained in a batch synthesis.

Subsequently, *in vitro* protein synthesis was performed with ^{35}S-methionine both in vesicles and in batch using the identical aforementioned DNA mixture, and the quantity of synthesized protein was estimated from the band intensity of the corresponding band obtained from autoradiography of the SDS polyacrylamide gel. We found that the ratio of synthesized GFP and EmrE was not affected by the difference in the reaction compartment (Figure 2c). Because there was no significant difference between the yield of GFP in GUVs and in batch (Figure 2a,b), this result suggests that the yield of EmrE in GUVs and in batch also did not differ. Therefore, N_{total} can be written as follows: $N_{total} = [E]_0V$, where $[E]_0$ is the concentration of EmrE obtained in a batch synthesis. We determined $[E]_0$ at different DNA concentrations by performing protein synthesis using ^{35}S-Met and quantifying the corresponding band from the autoradiograph obtained from SDS-PAGE (Figure 3a). Accordingly, we obtained N_{total} and plotted the relationship between N_{total} and N_{myc} (Figure 3b).

In vitro protein synthesis in vesicles and in batch has been reported to proceed differently in previous studies.[14,15,26] The discrepancy between these and our results remains unclear. Nevertheless, it is important to note that with the method we used[24] no significant difference was observed between reactions in vesicles and in batch; this result is consistent with the previous report[24] and thus is reproducible.

On the basis of the N_{total} and N_{myc} of vesicles with volume V, we estimated (1) the surface density of the integrated EmrE and (2) the fraction of membrane-integrated EmrE (i.e., $f = N_{myc}/N_{total}$), and we investigated the dependence of these parameters on vesicle volume.

Dependence of EmrE Integration on Vesicle Volume. The density of integrated EmrE on the membrane was estimated (Figure 4). Assuming the vesicle is a sphere, which is reasonable (Figures 1c and 5a),[27] the surface area (A) of the vesicle was calculated from V, and the density was determined knowing the value of N_{myc}. The density of EmrE was dependent on the DNA concentration used for the synthesis but not on the volume of the vesicle (Figure 4, inset). At the maximum DNA concentration used (3 nM), the surface density of the EmrE on the GUV membrane was approximately 300 molecules/μm^2 (Figure 4b), whereas that of the membrane proteins of an *E. coli* cell[28] is approximately $10^5/\mu$m^2. The GUVs contained 1000-fold lower membrane protein density than *E. coli*, implying that GUVs possess a large capacity for accommodating additional membrane proteins.

To support these FCM results, we acquired confocal microscopic images of the vesicles stained with a fluorescent antibody (Figure 5a) and performed a quantitative analysis (Figure 5b). First, we found that very few vesicles aggregated, indicating that the presented FCM analysis is that of isolated vesicles and not aggregates (Figure 5a). Second, we investigated the relationship between the observed vesicle area and the average fluorescence intensity of the membrane stained with a fluorescently labeled antibody (Figure 5b) and found that the variation in the fluorescence intensity is very large and ranges

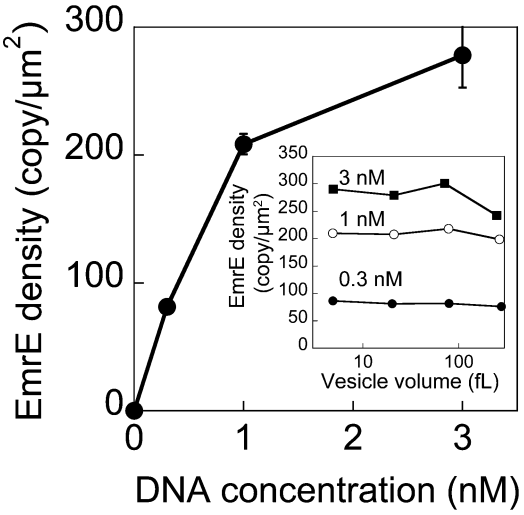

Figure 4. Relationship between the concentration of EmrE-encoding DNA used for protein synthesis and the surface density of EmrE on the GUV membrane. First, using the data shown in Figure 3b, the vesicles were classified into groups with V values of 2.15−10, 10−46.4, 46.4−215, and 215−1000 fL. Subsequently, the median value of $\langle N_{myc}\rangle$ and $\langle V\rangle$ for each group was calculated. The surface density was then obtained by calculating $\langle N_{myc}\rangle/\langle V\rangle$, assuming that the GUV is a sphere. The inset shows that the EmrE density was similar in vesicles of all volumes for a given DNA concentration. The densities at different volumes (inset) were averaged, and the relationship between the EmrE density and the DNA concentration used for the synthesis was plotted.

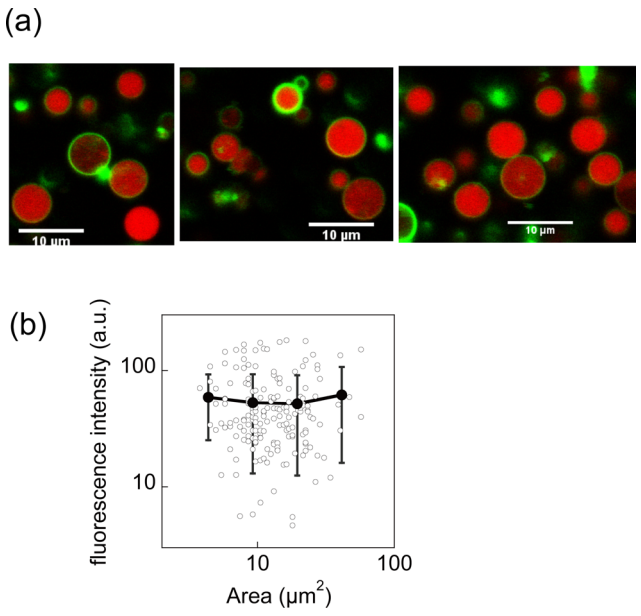

Figure 5. EmrE-expressing GUVs visualized by fluorescence confocal microscopy and their quantitative analysis. (a) Three representative images. Green fluorescence is derived from the AF488-labeled anti-myc antibody, and red fluorescence is derived from the TA647. (b) Relationship between the observed vesicle area and the average fluorescence intensity on the membrane obtained from the data shown in panel a. Open circles indicate the raw data, and the closed circles indicate the averages. Average values were obtained by classifying the vesicles into groups with area values of 3−6.34, 6.34−13.42, 13.42−28.37, and 28.37−60 μm^2 and then calculating the value of each group.

dx.doi.org/10.1021/sb400094c | *ACS Synth. Biol.* 2014, 3, 372−379

by approximately 50-fold. Nevertheless, the average intensity was not significantly different among different vesicle sizes. The results obtained from the microscopic images were consistent with those from the FCM analysis (Figure 4). Note that the images were acquired using a confocal microscope and thus the obtained vesicle area corresponded to the slice obtained at an arbitrary position on the vesicle.

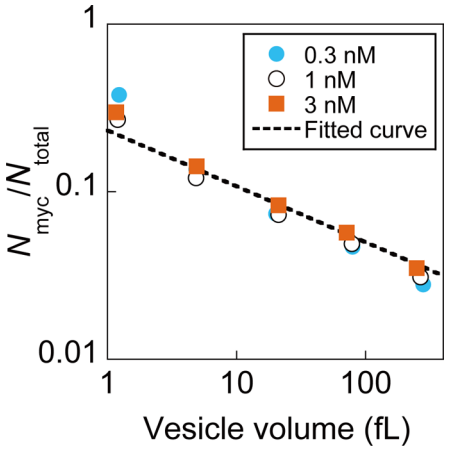

Figure 6. Dependence of the f (which is N_{myc}/N_{total}) value on vesicle volume. The results indicate that the fraction of membrane-integrated EmrE depended on the vesicle volume but not on the concentration of DNA used to synthesize EmrE. First, using the results in Figure 3b, the vesicles were classified into groups with V values of 0.464−2.15, 2.15−10, 10−46.4, 46.4−215, and 215−1000 fL. Subsequently, the median values of $\langle f \rangle$ and $\langle V \rangle$ for each group were calculated. The data were fitted to the curve generated by the equation $\log\langle f \rangle = (-1/3) \log\langle V \rangle + c$, where c is the fitting parameter. The fit using $\log\langle f \rangle = n \log\langle V \rangle + c$, where n and c are the fitting parameters, resulted in values of $n = -0.41$ and $c = -0.53$.

Subsequently, the dependence of $f = N_{myc}/N_{total}$ on vesicle volume was investigated (Figure 6). In vesicles with a volume of 1 fL, approximately 20% of the EmrE was integrated into the membrane with the myc-tag facing outward. The membrane-integrated fraction, f, decreased with larger values of V. In addition, f depended only on V, not on $[E]_0$ or the DNA concentration used for the synthesis. These trends, the constant surface density of EmrE with a defined DNA concentration (Figure 4), and the linearity between f and V in the log−log plot (Figure 6) can be explained by the presence of more lipids per unit volume in smaller vesicles (i.e., an increase in the surface-area-to-volume ratio).

Modeling the EmrE Membrane Integration. The utilized GUVs can be approximated to a sphere.[27] Therefore, the concentration of the lipid, [L], inside a vesicle with volume V and surface area A can be written as follows

$$[L] = \frac{\eta A}{V} = cV^{-1/3}$$

$$c = 3\eta\left(\frac{3}{4\pi}\right)^{-1/3} \quad (1)$$

where η is the molar amount of the lipid per unit area. Thus, the lipid concentration linearly correlates with the surface-area-to-volume ratio and increases with decreasing volume.

We then assumed the following two irreversible reactions involving EmrE (E)

$$E \xrightarrow{k_1} Agg$$

$$E + L \xrightarrow{k_2} EL$$

with a rate constant of k_1 and k_2, respectively, where the first equation represents the aggregation of EmrE inside the vesicle (which is a first-order reaction), and the second equation represents EmrE binding to the membrane and successful integration (which is a second-order reaction). From eq 1, f can be written as follows

$$f = \frac{N_{myc}}{N_{total}} = \frac{[EL]}{[E]_0} = \frac{[EL]}{[Agg] + [EL]} = \frac{k_2[E][L]}{k_1[E] + k_2[E][L]} = \frac{[L]}{K + [L]}$$

When assuming $k_1/k_2 = K \gg [L]$, and from eq 1, we obtain the following

$$f = \frac{[L]}{K} = \frac{c}{K}V^{-1/3} = \frac{c\left(\frac{4\pi}{3}\right)^{-1/3}}{K}\left(\frac{1}{r}\right) \quad (2)$$

This equation indicates that the fraction of membrane-integrated EmrE is linearly correlated with the lipid concentration (the first line of eq 2) or the membrane curvature, $1/r$ (the third line of eq 2), where r is the radius of the vesicle. Furthermore, N_{myc} and N_{total} can be written as follows

$$N_{total} = \left(\frac{K}{c}\right)^{3/2}[E]_0^{-1/2}(N_{myc})^{3/2} \quad (3)$$

$$\frac{N_{myc}}{A} = \frac{c}{K}[E]_0(4\pi)^{-1/3}3^{-2/3} \quad (4)$$

For the derivation of the equations, see the Supporting Information. Equation 2 predicts that the log−log plot of V versus f would have a slope of $-1/3$ (Figure 6). Equation 3 predicts that the log−log plot of N_{myc} versus N_{total} would have a slope of $3/2$ (Figure 3b). Equation 4 predicts that the surface density of EmrE would depend on the DNA concentration used for the synthesis but not the vesicle volume (Figure 4, inset). All equations were in agreement with the obtained results (Figures 3c, 4, and 6; dashed lines).

The agreement between the model and the results indicates that the observed trends in membrane integration can be described by the increase in the lipid concentration in smaller vesicles. However, the lipid concentration, [L], is linearly correlated with the membrane curvature, $1/r$ (eq 2). It is clear that f is dependent on the surface-area-to-volume ratio; however, whether the volume dependence of f is caused by the difference in [L] or $1/r$ of the vesicles cannot be distinguished. Nevertheless, we believe that the effect of [L] was much larger than that of $1/r$ because the linearity between f and [L] can be understood by the law of mass action, whereas there is no mechanism to describe the linearity between f and $1/r$. Although the confined reaction volume can produce various effects on intravesicular reactions,[15,29−34] we have

dx.doi.org/10.1021/sb400094c | ACS Synth. Biol. 2014, 3, 372−379

demonstrated for the first time that the surface-area-to-volume ratio has an important effect on membrane protein integration.

Conclusions. IVTTs have been used to study the interaction between membrane proteins and lipid vesicles. For example, the phospholipid composition of the lipid was shown to have a large effect on the membrane binding or association of the membrane protein,[35,36] whereas the number of transmembrane domains of the proteins was shown to not correlate with the efficiency of membrane association.[37,38] Despite the many studies that have been conducted, no previous study has demonstrated the dependence of vesicle size on membrane protein integration. We initially investigated this aspect using the simplest lipid composition (i.e., 100% POPC). Using POPC vesicles, we found that the fraction of EmrE that integrated into the membrane increased with decreasing vesicle volume.

The PURE system lacks translocases, which are the machinery required for the *in vivo* membrane integration of EmrE.[39] Nevertheless, at least 20% of the synthesized EmrE was integrated into the membrane of 1 fL GUVs; twice as much could have been integrated if we assume that all membrane-integrated EmrE molecules existed as dimers. The reason for the discrepancy between *in vitro* and *in vivo* membrane integration remains unclear. There are several reports on the integration of proteins into the naked membrane using IVTTs.[3,4] The mechanism of the insertion remains to be elucidated;[40,41] however, because of its simplicity, membrane insertion using IVTT is a useful tool to clarify the basic properties of membrane protein integration.[42,43] Although most of the previous studies used *in vitro* protein synthesis outside the vesicle,[3,4] our method enables the analysis of protein integration from the inside. Beyond traditional strategies for studying membrane integration in which the membrane integration of proteins is detected by the protection of proteins from proteases,[43,44] our method that uses GUV and FCM can be employed to investigate further the mechanism of membrane protein integration. Furthermore, the experimental setup described herein may be used for the *in vitro* evolution of membrane proteins,[19] which could advance the field of membrane protein engineering.

METHODS

Plasmid Construction. The plasmids encoding EmrE (pET-EmrE-myc and pET-EmrE-FLAG) were constructed from the plasmids pCAN24N-emrE (NBRP, Shizuoka, Japan) and pET-gusA[45] using PCR and an In-Fusion HD kit (Takara, Shiga Japan) according to the manufacturer's instructions. The vectors pET-EmrE-myc and pET-EmrE-FLAG encoded EmrE with a C-terminal myc tag and EmrE with a FLAG tag, respectively, which was under the control of the T7 promoter. Site-directed mutagenesis was used to construct pET-E14C-myc from pET-EmrE-myc. PCR was performed using KOD FX and DNA polymerase (Toyobo, Osaka, Japan) according to the manufacturer's instructions unless otherwise noted. The template DNA used for the *in vitro* transcription−translation system (IVTT) was prepared using PCR and pET-G5tag (which encoded GFP), pET-EmrE-myc, or pET-E14C-myc as a template; the primers T7F (5′-TAATACGACTCA-CTATAGGG-3′) and T7R (5′-GCTAGTTATTGCTCA-GCGG-3′) were used for the reaction. The PCR product was purified using a QIAquick PCR purification kit (Qiagen, Hilden, Germany) according to the manufacturer's instructions.

Preparation of Cell-Sized Vesicles. The IVTT used in this study was a reconstituted *in vitro* translation system (the PURE system) prepared in the laboratory.[46] Vesicles containing the PURE system were prepared using the w/o emulsion-transfer method,[23,27] as described in our previous report.[24] Briefly, 20 μL of the PURE system supplemented with the template DNA, 200 mM sucrose, 0.8 U/μL of RNase inhibitor (RNasin Plus; Promega, Madison, WI), and 1 μM transferrin Alexa Fluor 647 conjugate (TA647; Life Technologies, Carlsbad, CA) was added to 200 μL of liquid paraffin (Wako Pure Chemical Industries, Osaka, Japan) containing 2 mg of POPC (Avanti Polar Lipids, Alabaster, AL). The mixtures were vortexed for 30 s to form w/o emulsions that were then equilibrated on ice for 10 min. An aliquot of 200 μL of this solution was gently placed on top of 200 μL of the outer solution (see below for the composition) and was centrifuged at 18 000*g* for 20 min at 4 °C. The pelleted GUVs were collected through an opening at the bottom of the tube. The collected GUVs were pelleted once again by centrifugation at 18 000*g* for 20 min at 4 °C and were suspended in fresh outer solution. Protein synthesis inside the GUVs was conducted at 37 °C for 3 h. The outer solution contained the low-molecular-weight components of the PURE system (0.3 mM of each amino acid, 3.75 mM ATP, 2.5 mM GTP, 1.25 mM CTP and UTP, 1.5 mM spermidine, 25 mM creatine phosphate, 1.5 mM dithiothreitol (DTT), 0.02 μg/μL 10-formyl-5,6,7,8-tetrahydrofolic acid, 280 mM potassium glutamate, 18 mM $Mg(OAc)_2$, and 100 mM HEPES (pH 7.6)) supplemented with 200 mM glucose.

FACS Analysis. To detect myc-tagged EmrE displayed on the vesicles, an anti-myc-tag antibody conjugated to AF488 (MBL, Japan) was added (final concentration of 5 μg/mL) to the vesicle suspension, which was incubated at 37 °C for 30 min. The unbound antibody was removed by pelleting the vesicles via centrifugation at 18 000*g* for 5 min and resuspending the pellet in dilution buffer (100 mM HEPES-KOH (pH 7.6), 280 mM potassium glutamate, 18 mM $Mg(OAc)_2$, and 200 mM glucose). The resulting vesicle suspension was analyzed using FCM. To detect the influx of EtBr, the external solution of the vesicle was replaced with a buffer that was identical to the dilution buffer but contained 0.5 μg/mL of EtBr at a pH of 6.8 or 8.1.

The fluorescent signals from AF488, GFP, EtBr, and TA647 were measured using FACS (FACSAria II; BD Biosciences, Franklin Lakes, NJ). All analyses were conducted with the vesicle population defined as GUVs based on the 2D plot of forward- and side-scattering intensities, as in our previous reports.[24] AF488 and EtBr were excited with a 488 nm semiconductor laser, and the emission was detected through 530 ± 15 and 616 ± 11 nm band-pass filters, respectively. TA647 was excited with a HeNe laser (633 nm), and the emission was detected through a 660 ± 10 nm band-pass filter. The total fluorescence intensity of the 100 000 GUVs was measured and subjected to analysis. The aqueous volume of the GUVs (V [fL]) was estimated from the TA647 fluorescence intensity (FI_{647}) using the correlation between the FI_{647} and the number of Alexa Fluor 647 molecules obtained using calibration beads (Quantum Alexa Fluor 647 MESF, Bangs Laboratories, Inc.) and from the average number of Alexa Fluor 647 molecules coupled to each transferrin molecule. The number of anti-myc antibodies bound to each vesicle (N_{myc}) was estimated from the AF488 fluorescence intensity using the correlation between the AF488 fluorescence intensity and the

dx.doi.org/10.1021/sb400094c | *ACS Synth. Biol.* 2014, 3, 372−379

number of AF488 molecules obtained using calibration beads (Quantum Alexa Fluor 488 MESF, Bangs Laboratories, Inc.) and from the average number of AF488 molecules (5.2) coupled to each antimyc antibody.

Microscopy. Microscopy images shown in Figure 1 were obtained using an inverted light microscope (BX50; Olympus, Japan) equipped with an EM-CCD camera (ADT-100; Flovel, Japan) using a 60× oil immersion objective. Fluorescence images of EtBr and AF488 were obtained through corresponding filters and dichroic mirror units (WIG and NIBA; Olympus).

Microscopic images shown in Figure 5 were obtained using confocal laser scanning microscope (Leica TCS SP8; Leica microsystems, Tokyo, Japan) using a 100× oil immersion objective. Images for the AF488 ligand and TA647 were obtained using a 488 nm excitation laser and hybrid detector set to 474−607 nm. The relationship between the vesicle area and the fluorescence intensity of the membrane was obtained as follows. First, the average TA647 fluorescence per unit area of approximately 300 vesicles was quantified, resulting in a bimodal distribution. The vesicle population with higher fluorescence (i.e., with a TA647 fluorescence intensity higher than 100 (a.u.)) was used for further analysis. This treatment removed the non-vesicle-like particles. We then measured the fluorescence of the membrane (average value of three arbitrary positions) for each vesicle and plotted the relationship between the vesicle area and the fluorescence signal from the membrane.

■ ASSOCIATED CONTENT

Supporting Information

Equations for modeling the EmrE membrane integration for the density of membrane-integrated EmrE. Histogram of EtBr fluorescence/vesicle volume for the data shown in Figure 1b. This material is available free of charge via the Internet at http://pubs.acs.org.

■ AUTHOR INFORMATION

Corresponding Author

*Tel: 81-6-6879-4172; Fax: 81-6-6879-7428; E-mail: matsuura_tomoaki@bio.eng.osaka-u.ac.jp.

Author Contributions

H.S. and S.F. performed the experiments. T.Y. provided the PURE system. H.S., T.M., Y.K., and H.W. analyzed the data. H.S. and T.M. wrote the paper.

Notes

The authors declare no competing financial interest.

■ ACKNOWLEDGMENTS

We thank Dr. Yasuaki Kazuta for providing the PURE system and Dr. Atsuko Uyeda for technical assistance.

■ REFERENCES

(1) Yildirim, M. A., Goh, K. I., Cusick, M. E., Barabasi, A. L., and Vidal, M. (2007) Drug-target network. *Nat. Biotechnol. 25*, 1119−1126.

(2) Stevens, T. J., and Arkin, I. T. (2000) Do more complex organisms have a greater proportion of membrane proteins in their genomes? *Proteins 39*, 417−420.

(3) Katzen, F., Peterson, T. C., and Kudlicki, W. (2009) Membrane protein expression: No cells required. *Trends Biotechnol. 27*, 455−460.

(4) Schwarz, D., Dotsch, V., and Bernhard, F. (2008) Production of membrane proteins using cell-free expression systems. *Proteomics 8*, 3933−3946.

(5) Carlson, E. D., Gan, R., Hodgman, C. E., and Jewett, M. C. (2012) Cell-free protein synthesis: Applications come of age. *Biotechnol. Adv. 30*, 1185−1194.

(6) Bay, D. C., Rommens, K. L., and Turner, R. J. (2008) Small multidrug resistance proteins: A multidrug transporter family that continues to grow. *Biochim. Biophys. Acta 1778*, 1814−1838.

(7) Noireaux, V., and Libchaber, A. (2004) A vesicle bioreactor as a step toward an artificial cell assembly. *Proc. Natl. Acad. Sci. U.S.A. 101*, 17669−17674.

(8) Noireaux, V., Bar-Ziv, R., Godefroy, J., Salman, H., and Libchaber, A. (2005) Toward an artificial cell based on gene expression in vesicles. *Phys. Biol. 2*, P1−8.

(9) Maeda, Y. T., Nakadai, T., Shin, J., Uryu, K., Noireaux, V., and Libchaber, A. (2012) Assembly of MreB filaments on liposome membranes: A synthetic biology approach. *ACS Synth. Biol. 1*, 53−59.

(10) Antonny, B. (2011) Mechanisms of membrane curvature sensing. *Annu. Rev. Biochem. 80*, 101−123.

(11) Ramamurthi, K. S. (2010) Protein localization by recognition of membrane curvature. *Curr. Opin. Microbiol. 13*, 753−757.

(12) Shapiro, L., McAdams, H. H., and Losick, R. (2009) Why and how bacteria localize proteins. *Science 326*, 1225−1228.

(13) Sunami, T., Kita, H., Hosoda, K., Matsuura, T., Suzuki, H., and Yomo, T. (2009) Detection and analysis of protein synthesis and RNA replication in giant liposomes. *Methods Enzymol. 464*, 19−30.

(14) Saito, H., Kato, Y., Le Berre, M., Yamada, A., Inoue, T., Yosikawa, K., and Baigl, D. (2009) Time-resolved tracking of a minimum gene expression system reconstituted in giant liposomes. *ChemBioChem 10*, 1640−1643.

(15) Kato, A., Yanagisawa, M., Sato, Y. T., Fujiwara, K., and Yoshikawa, K. (2012) Cell-sized confinement in microspheres accelerates the reaction of gene expression. *Sci. Rep. 2*, 283-1−283-5.

(16) Sunami, T., Sato, K., Matsuura, T., Tsukada, K., Urabe, I., and Yomo, T. (2006) Femtoliter compartment in liposomes for in vitro selection of proteins. *Anal. Biochem. 357*, 128−136.

(17) Nishikawa, T., Sunami, T., Matsuura, T., Ichihashi, N., and Yomo, T. (2012) Construction of a gene screening system using giant unilamellar liposomes and a fluorescence-activated cell sorter. *Anal. Chem. 84*, 5017−5024.

(18) Nishikawa, T., Sunami, T., Matsuura, T., and Yomo, T. (2012) Directed evolution of proteins through in vitro protein synthesis in liposomes. *J. Nucleic Acids 2012*, 923214-1−923214-11.

(19) Fujii, S., Matsuura, T., Sunami, T., Kazuta, Y., and Yomo, T. (2013) In vitro evolution of alpha-hemolysin using a liposome display. *Proc. Natl. Acad. Sci. U.S.A. 110*, 16796−16801.

(20) Shimizu, Y., Inoue, A., Tomari, Y., Suzuki, T., Yokogawa, T., Nishikawa, K., and Ueda, T. (2001) Cell-free translation reconstituted with purified components. *Nat. Biotechnol. 19*, 751−755.

(21) Morrison, E. A., DeKoster, G. T., Dutta, S., Vafabakhsh, R., Clarkson, M. W., Bahl, A., Kern, D., Ha, T., and Henzler-Wildman, K. A. (2012) Antiparallel EmrE exports drugs by exchanging between asymmetric structures. *Nature 481*, 45−50.

(22) Nishino, K., and Yamaguchi, A. (2001) Analysis of a complete library of putative drug transporter genes in *Escherichia coli*. *J. Bacteriol. 183*, 5803−5812.

(23) Pautot, S., Frisken, B. J., and Weitz, D. A. (2003) Production of unilamellar vesicles using an inverted emulsion. *Langmuir 19*, 2870−2879.

(24) Nishimura, K., Matsuura, T., Nishimura, K., Sunami, T., Suzuki, H., and Yomo, T. (2012) Cell-free protein synthesis inside giant unilamellar vesicles analyzed by flow cytometry. *Langmuir 28*, 8426−8432.

(25) Yerushalmi, H., and Schuldiner, S. (2000) An essential glutamyl residue in EmrE, a multidrug antiporter from *Escherichia coli*. *J. Biol. Chem. 275*, 5264−5269.

(26) Nourian, Z., Roelofsen, W., and Danelon, C. (2012) Triggered gene expression in fed-vesicle microreactors with a multifunctional membrane. *Angew. Chem., Int. Ed. 51*, 3114−3118.

(27) Nishimura, K., Hosoi, T., Sunami, T., Toyota, T., Fujinami, M., Oguma, K., Matsuura, T., Suzuki, H., and Yomo, T. (2009) Population

analysis of structural properties of giant liposomes by flow cytometry. *Langmuir 25*, 10439−10443.
(28) Phillips, R., Kondev, J., and Theriot, J. (2009) *Physical Biology of the Cell*, Garland Science, New York.
(29) Matsuura, T., Hosoda, K., Kazuta, Y., Ichihashi, N., Suzuki, H., and Yomo, T. (2012) Effects of compartment size on the kinetics of intracompartmental multimeric protein synthesis. *ACS Synth. Biol. 1*, 431−437.
(30) Bansho, Y., Ichihashi, N., Kazuta, Y., Matsuura, T., Suzuki, H., and Yomo, T. (2012) Importance of parasite RNA species repression for prolonged translation-coupled RNA self-replication. *Chem. Biol. 19*, 478−487.
(31) Urabe, H., Ichihashi, N., Matsuura, T., Hosoda, K., Kazuta, Y., Kita, H., and Yomo, T. (2010) Compartmentalization in a water-in-oil emulsion repressed the spontaneous amplification of RNA by Q beta replicase. *Biochemistry 49*, 1809−1813.
(32) Lizana, L., Konkoli, Z., Bauer, B., Jesorka, A., and Orwar, O. (2009) Controlling chemistry by geometry in nanoscale systems. *Annu. Rev. Phys. Chem. 60*, 449−468.
(33) Okano, T., Matsuura, T., Suzuki, H., Yomo, T. (2013) Cell-free protein synthesis in a microchamber revealed the presence of an optimum compartment volume for high-order reactions. *ACS Synth. Biol.* [Online early access]. DOI: 10.1021/sb400087e. Published Online: Aug 30.
(34) Tsuji, A., and Yoshikawa, K. (2010) On-off switching of transcriptional activity of large DNA through a conformational transition in cooperation with phospholipid membrane. *J. Am. Chem. Soc. 132*, 12464−12471.
(35) Nomura, S. M., Kondoh, S., Asayama, W., Asada, A., Nishikawa, S., and Akiyoshi, K. (2008) Direct preparation of giant proteo-liposomes by in vitro membrane protein synthesis. *J. Biotechnol. 133*, 190−195.
(36) Kalmbach, R., Chizhov, I., Schumacher, M. C., Friedrich, T., Bamberg, E., and Engelhard, M. (2007) Functional cell-free synthesis of a seven helix membrane protein: in situ insertion of bacterio-rhodopsin into liposomes. *J. Mol. Biol. 371*, 639−648.
(37) Katzen, F., Fletcher, J. E., Yang, J. P., Kang, D., Peterson, T. C., Cappuccio, J. A., Blanchette, C. D., Sulchek, T., Chromy, B. A., Hoeprich, P. D., Coleman, M. A., and Kudlicki, W. (2008) Insertion of membrane proteins into discoidal membranes using a cell-free protein expression approach. *J. Proteome Res. 7*, 3535−3542.
(38) Nozawa, A., Ogasawara, T., Matsunaga, S., Iwasaki, T., Sawasaki, T., and Endo, Y. (2011) Production and partial purification of membrane proteins using a liposome-supplemented wheat cell-free translation system. *BMC Biotechnol. 11*, 35-1−35-10.
(39) Tate, C. G. (2010) Membrane protein gymnastics. *Science 328*, 1644−1645.
(40) Nishiyama, K., Ikegami, A., Moser, M., Schiltz, E., Tokuda, H., and Muller, M. (2006) A derivative of lipid A is involved in signal recognition particle/SecYEG-dependent and -independent membrane integrations. *J. Biol. Chem. 281*, 35667−35676.
(41) Kawashima, Y., Miyazaki, E., Muller, M., Tokuda, H., and Nishiyama, K. (2008) Diacylglycerol specifically blocks spontaneous integration of membrane proteins and allows detection of a factor-assisted integration. *J. Biol. Chem. 283*, 24489−24496.
(42) Nishiyama, K., Maeda, M., Abe, M., Kanamori, T., Shimamoto, K., Kusumoto, S., Ueda, T., and Tokuda, H. (2010) A novel complete reconstitution system for membrane integration of the simplest membrane protein. *Biochem. Biophys. Res. Commun. 394*, 733−736.
(43) Nishiyama, K., Maeda, M., Yanagisawa, K., Nagase, R., Komura, H., Iwashita, T., Yamagaki, T., Kusumoto, S., Tokuda, H., and Shimamoto, K. (2012) MPIase is a glycolipozyme essential for membrane protein integration. *Nat. Commun. 3*, 1260-1−1260-10.
(44) Kuruma, Y., Nishiyama, K., Shimizu, Y., Muller, M., and Ueda, T. (2005) Development of a minimal cell-free translation system for the synthesis of presecretory and integral membrane proteins. *Biotechnol. Prog. 21*, 1243−1251.
(45) Matsuura, T., Hosoda, K., Ichihashi, N., Kazuta, Y., and Yomo, T. (2011) Kinetic analysis of beta-galactosidase and beta-glucuronidase tetramerization coupled with protein translation. *J. Biol. Chem. 286*, 22028−22034.
(46) Matsuura, T., Kazuta, Y., Aita, T., Adachi, J., and Yomo, T. (2009) Quantifying epistatic interactions among the components constituting the protein translation system. *Mol. Syst. Biol. 5*, 297-1−297-10.